Published in Plant Electrophysiology, p. 127-144
DOI: 10.1007/978-3-642-29119-7_5

Springer Verlag https://doi.org/10.1007/978-3-642-29119-7_5

Intracellular Measurements of the Electrical Properties of Walled Cells.

Roger R. Lew
York University
Department of Biology
Toronto, Canada

Abstract
The electrical properties of plant (and other walled) cells have a tremendous impact on the transport of ions into or out of the cell. Ion transport is necessary for plant growth and survival. Thus, the electrical properties of the plant cell are crucial to the survival and growth of the plant. The most direct way to measure the electrical properties of the cell is intracellular impalement with a microelectrode. A range of techniques, their execution and potential pitfalls are described in this chapter. Special attention is paid to dual impalement techniques to measure current-voltage relations of the cell.

1 Intracellular measurements in intact, turgid walled cells

The foundation of the 'electrical' plant is the electrical nature of individual cells. To measure the electrical properties of walled cells, the most direct technique is to impale the cell with a microelectrode so that the electrical potential inside of the cell can be compared with the outside potential: The *trans-membrane* potential. Impalements can be done relatively easily on large cells, such as Characean giant algal cells that have dimensions of 1.5 mm by 3 cm. They are far more challenging to perform on small cells of higher plants —20 μm by 40 μm— and fungi with hyphal diameters of <15 μm. Etherton and Higinbotham (1960) and Slayman and Slayman (1962) successfully measured the potentials of barley and fungal cells, respectively. They showed that respiratory inhibitors depolarized the negative-inside potential of the cell, demonstrating that the *trans-membrane* potential required cellular metabolic energy, that is, the potential is actively generated. Since these pioneering measurements, the electrophysiological properties of numerous walled cells have been studied. Because the *trans-membrane* potential strongly influences ion uptake and release, it is fundamental to transport energetics and kinetic mechanisms. Even the transport of uncharged solutes is often coupled with transport of charged ions (usually H^+). Ion and solute transport are crucial to the survival and growth of the organism because of their impact on nutrition. Therefore, the electrical properties of a cell are crucial for survival and growth.

In this chapter, I will describe methods for intracellular measurements used to characterize the *trans-membrane* potential and other electrical properties of walled cells. I will introduce the technique and then describe the electrical properties of the cell. Finally, I will explore more sophisticated techniques, such as voltage clamp, which reveals the voltage dependence of *trans–membrane* ionic currents.

1.1 The basics of intracellular measurements.

There are a number of books that describe intracellular measurements of the electrical properties of cells. Microelectrode construction and use are described by Thomas (1978), Purves (1981) and Blatt (1991). Ion-selective microelectrodes are described by Ammann

(1986). The Plymouth Workshop Handbook (Ogden 1994) includes contributed chapters describing a variety of experimental techniques and analysis.

Impaling a cell with a microelectrode first requires fabrication of the micropipette. Details of fabrication techniques have been described extensively by Purves (1981). The micropipette tip must be sharp, with a diameter small enough so that it can penetrate the wall and plasma membrane with minimal damage to the cell. Micropipettes are fabricated using pipette pullers. These are commercially available from a number of vendors. A schematic of the technique is shown in Figure 1. Briefly, a short length of capillary tubing is held at both ends (the upper end is fixed, the lower end is attached to a heavy weight), and a localized region at the center of the tube heated until the glass has softened. The weight slowly drops, stretching the glass tube, followed by a fast pull using a solenoid that separates the two ends of the capillary. The resulting tip is quite sharp, with dimensions in the range of 200–500 nm. Once pulled, the inside of the micropipette is filled with electrolyte (3 M KCl is commonly used). The electrolyte creates an electrically conductive pathway that is required for electrical measurements. Capillary tubing for micropipette fabrication contains an internal fiber that improves the ability to fill the very small bore at the sharp tip of the micropipette with the salt solution — avoiding air bubbles that would block electrical conductivity. The chloride ions in the KCl backfill solution function as part of an Ag-AgCl half-cell to connect the micropipette to an electrometer to measure the voltage. Silver chloride coating on the silver wire reacts *reversibly* with chloride ions in solution ($Ag + Cl^- <—> AgCl + e^-$) to create the electrical connection to the electrometer. A similar half-cell is connected to the extracellular solution with a salt bridge (usually 3 M KCl in agar) to form an electrical ground that completes the circuit to the electrometer.

Because of the small dimensions of the micropipette tip, its resistance is very high (in the range of $20–40 \times 10^6\ \Omega$). At such a high resistance, electrical noise from external sources can obscure the measured potentials, which is why the measuring apparatus is usually shielded from the external environment by a grounded metal enclosure known as a Faraday cage. The high resistance also requires that the voltage be measured with a high input impedance electrometer.

Impaling a small cell requires micromanipulators and isolation from mechanical vibration. Micromanipulators use mechanical, hydraulic, or piezoelectric mechanisms to allow fine positional control of the microelectrode tip at resolutions less than 1 micron. Both commercial and ‘home-made’ vibration isolation systems rely on a heavy (high inertia) tabletop made of metal or granite resting on top of ‘shock absorbers’ (pressurized air cylinders are commonly used).

Examples of impalements into algal, fungal and plant cells are shown in Figure 2. The cell diameters range from 8 to 100 microns. In all cases, the tip must puncture the wall, shown in Figure 2A where the micropipette tip bends before it ‘pops’ into the cell (the green alga *Eremosphaera viridis*). In Figure 2B, the fact that the puncture site is sealed against high pressure is demonstrated by the burst of cytoplasm out of the cell when the tip is removed (the fungus *Neurospora crassa*). That cells survive impalement quite well is demonstrated in Figure 2C, in which the root hair (the higher plant *Arabidopsis thaliana*) continues growing after impalement. For the fungal and plant impalements, the electrical traces demonstrate another property of the impalement. In both cases, the cell was impaled with a *second* micropipette at the vertical arrows. The second impalement had no effect on the measured potential (after a transient and small depolarization), indicating how well the micropipettes are sealed electrically. If there were significant

damage and ion leakage at the impalement sites, the potential would have become depolarized, and remained depolarized.

Having impaled the cell, what are the electrical properties?

1.2 Electrical network of a walled cell.

The terms common to electronics —voltage, current, resistance and capacitance—also describe the electrical properties of cells. The electrical network for an idealized walled cell incorporating these elements is shown in Figure 3. Voltage, current and resistance are related through Ohm's Law: V = IR, where V is the voltage (in Volts), I is the current (in Amperes) and R is the resistance (in Ohms, Ω). Typical values for a walled cell are a 'resting potential' of –0.15 Volts (negative inside). The 'resting potential' indicates that the net current is zero. This means that, although ion fluxes will be occurring, there is no *net* charge movement across the membrane. A typical cell resistance is in the range of $10–20 \times 10^6$ Ω. Larger cells have lower resistance compared to smaller cells because the specific resistance is fairly constant (about 1.5 kΩ cm^2). Capacitance is a more complicated property. In simple terms, it is the ability (or capacity) of the cell to hold a net charge, similar to a battery. Cell capacitance is directly related to the area of plasma membrane at the cell boundary: the larger the cell, the higher the capacitance. The impact of capacitance is two-fold. It affects how much of a net charge imbalance between the inside and outside of the cell is required to create the trans-membrane potential. Net charge (Q, in Coulombs) is the product of the capacitance (C, Farads, or coulombs $volt^{-1}$) and the potential difference (ΔE, volts): $Q = C \bullet \Delta E$. For biological membranes, specific capacitance is about 10^{-2} F m^{-2}; the specific capacitance is multiplied by cell area to obtain the capacitance. The charge can also be defined by the concentration of net charges. That is, the net charge (Q) is the product of the cell volume (V, in m^3), the net concentration of the ion (c_{ion}, in mole m^{-3}) and the Faraday constant (F, 96480 coulombs $mole^{-1}$, to convert coulombs to moles): $Q = V \bullet c_{ion} \bullet F$. Combining the two equations and solving for the net ion concentration: $c_{ion} = (C \bullet \Delta E)/(V \bullet F)$. For a typical cell with dimensions of $20 \times 20 \times 80$ μm, a net charge concentration of 3.5×10^{-3} mole m^{-3} (3.5 μM) will create a potential of 150 mV. This is a very small charge difference compared to the usual ion concentrations of the cell (about 200 mM). The other effect of capacitance is related to the time it takes to charge the membrane capacitance. The higher the capacitance, the longer it takes for the potential to change in response to net ion flow into or out of the cell. This places limits on the measurability of fast events. Capacitance can be harnessed in some techniques that use a single micropipette to measure *both* the potential and resistance of the cell plasma membrane. For example, the discontinuous voltage clamp (described below) relies on differences in the capacitances of the electrode and cell (and therefore the time responses) to separate the resistance of the cell from the resistance of the microelectrode impaled into the cell.

To measure the full range of electrical properties of the cell, it is necessary to have some means of both injecting current and monitoring voltage (so that two if the three terms of Ohm's Law are known). One such method is the patch clamp technique (Hamill et al., 1981). Patch clamp revolutionized the study of ion transport in cells, including animal, fungal, algal and higher plant cells. The two major discoverers, Erwin Neher and Bert Sakmann were awarded the Nobel Prize in 1991. The power of the patch clamp technique was two-fold. First, it allowed individual ion channels to be measured *in situ*, in their natural state in the membrane. Second, with the whole cell mode, it enabled the experimenter to extend the range of possible measurements: to examine the voltage and time dependence of ionic currents and use this information to identify the specific ions

contributing to the current. With patch clamp, a wealth of information has been uncovered about the molecular foundations of ionic transport in cells.

There is a drawback to the use of patch clamping of plants, algae and fungi. When the patch clamp technique is used to measure ionic currents in walled cells, the wall must first be removed to expose the plasma membrane to the patch pipette. To avoid lysis, the cell must be held in a solution of osmolarity high enough to induce plasmolysis. This is necessary whether the wall is removed by enzymatic digestion or some other technique, such as laser ablation. This means that the advantage of patch clamp —to examine the voltage and time dependence of ion transport across the plasma membrane— is offset by the non-physiological condition of the cell: plasmolyzed and probably attempting turgor recovery. Certainly not growing, certainly in an abnormal physiological state, the plasmolyzed cell is a technical problem that can obscure the relevance of patch clamp measurements. The ideal way to overcome this is to perform measurements of the voltage and time dependence of ionic currents in intact, turgid, possibly even growing cells. But how can this be done in an intact cell?

2 Voltage clamping intact turgid cells

Voltage clamp is the technique of choice to measure the voltage and time dependence of ionic currents across the plasma membrane. There are three ways to voltage clamp intact turgid cells: discontinuous voltage clamp, dual impalements, and double barrel micropipettes. In all instances, the intent is to measure the voltage and time dependence of the plasma membrane ionic currents separate from any contribution of the micropipette itself. The micropipette resistance is a significant problem, because the resistance at the tip of the micropipette is often similar in magnitude to the resistance of the plasma membrane. This can cause an inability to separate the voltage and time dependence of ionic currents through the micropipette tip from the ionic currents through the plasma membrane.

2.1 Discontinuous voltage clamp: a single barrel used for both current injection and voltage monitoring

Finkel and Redman (1984) described the discontinuous single microelectrode voltage clamp technique. The technique has been used successfully in intact higher plant cells. The basic idea is that the time dependence of electrical currents at the microelectrode tip are very different from those of the plasma membrane because the capacitance of the micropipette tip is much lower than the capacitance of the cell membrane. This will cause a much faster time response, τ, defined as resistance (R) • capacitance (C): $\tau = R \bullet C$. By rapidly switching between current injection and voltage measurements, it is possible to separate *temporally* the contribution of the micropipette from the contribution of the plasma membrane, as long as $\tau_{electrode} < \tau_{cell}$. A set of papers using the discontinuous single electrode voltage clamp technique illustrates the technique and problems. Forestier et al. (1998) explored the use of the technique to identify slow anion currents in guard cells. The advantage of the technique was that measurements could be done in intact cells. Since guard cells change their turgor in response to different stimuli to control stomata aperture in the epidermis of the leaf, intact cells offer much greater insight into ion transport required for turgor changes compared to the turgor-less protoplasts used for patch clamp. In the discontinuous single electrode voltage clamp technique, it is necessary to electronically compensate for the capacitance of the electrode. Roelfsema et al. (2001) raised doubts about the applicability of the discontinuous single-electrode voltage clamp technique in small cells, like guard cells, because the low capacitance of

small cells would be similar to the capacitance of the electrode ($\tau_{electrode} \sim \tau_{cell}$); thus, a clear separation of the contribution of the electrode and cell would be difficult. Raschke et al. (2003) confirmed the results of Forestier et al. (1998), noting that it is crucial to use micropipettes that possess a linear current-voltage relation to assure that their capacitance can be compensated electronically. That is, the resistance must be voltage independent to assure R • C is constant for all clamped voltages. Although others have used this technique, the three papers cited above give a flavor of the doubts associated with the method. There are two issues: whether it is electronically possible to compensate for the electrode capacitance (or more accurately, time response, R • C) consistently, and whether the properties of the microelectrode tip are the same before and during insertion into the cell. In fact, Etherton et al. (1977) explored the latter question by directly comparing membrane resistance measurements obtained using two electrodes impaled separately into the same cell with single electrode impalements. They expressed the concern that the properties of the single electrode change upon impalement, rendering the technique questionable. Guard cells do not lend themselves to multiple impalements, so the discontinuous voltage clamp technique remains a useful technique to avoid the protoplasting required to patch clamp the cell, with caveats regarding the quality of the data. Supporting evidence, such as inhibitor effects (Forestier et al. 1998; Bouteau et al. 1999), bolsters interpretation of the data.

2.2 Dual impalements

Etherton et al. (1977) assumed that dual impalements with a voltage monitoring electrode and a current-injecting electrode were the “standard by which the accuracy” of single electrode techniques “could be judged”. Since the two processes, voltage monitoring and current injection, are separate, this is a likely assumption. One concern exists, that multiple impalements may affect the resistance of the plasma membrane due to membrane damage caused by the impalements, but Lew (2000) presented evidence discounting this possibility, at least in root hairs, by showing that multiple impalements do not cause a decrease in the potential, which means that the impalement site is not a source of significant ionic leakage. Supporting evidence is shown in Figure 2. Multiple impalements are technically difficult. The cells must be accessible, and good imaging is very helpful, to ensure the micropipettes are impaled into the same cellular compartment. Indeed, the 'standard' to assure where the tips are located is fluorescent dye injection (Holdaway-Clarke et al. 1996). Because only a single impalement into the cell is required, double barrel micropipettes offer technical advantages, while retaining separation of the voltage and current-injecting microelectrodes.

2.3 Double barrel micropipettes

A number of researchers have used double barrel micropipettes over the years. In fungi, Michael Blatt and others used them to perform voltage clamping of the filamentous fungus *Neurospora crassa* (Blatt and Slayman 1983, 1987). Blatt subsequently used the technique in guard cells (Blatt 1987) and wrote a primer on double barrel micropipettes and other electrophysiological techniques (Blatt 1991) that I recommend highly for new and experienced electrophysiologists.

3 Double barrel micropipette fabrication

The fabrication of double barrel micropipettes involves a sequential set of steps that are best performed by fabricating a batch of micropipettes at the same time. Borosilicate capillaries with internal filaments are first cut to an appropriate length (about 7 cm). We

use 1 mm OD, 0.58 mm ID tubing. The two capillaries are inserted into a micropipette puller in which one of the two clamps on either side of the heating filament can be rotated (Figure 4). When the heating filament has softened the glass, the capillaries are rotated 360º to create a twist in the glass. Then standard pulling protocols are used to pull the micropipette. Once pulled, a small amount of fast-setting epoxy is applied just above the twist to strengthen the fused joint between the two capillaries. Finally, one of the barrels is heated and pulled away to form a Y-shape. This eases insertion of one of the barrels of the micropipette into a holder, and insertion of a chlorided silver wire into the other barrel. Photographs of the fabrication steps are shown in Figure 4C.

Typically, we fabricate 8–10 of the double barrel micropipettes at the same time. First, all are pulled. Then epoxy is applied. When hardened, one barrel is pulled away to form a Y. Then they are stored in a covered dish until used. Fabrication takes about 1-2 hours.

One problem that can arise is crack formation in one of the glass barrels, probably during the twisting if the glass has not softened enough during heating. The cracks are not visible (except as a stress crack under magnification), but reveal themselves when the micropipettes are being tested for tip resistance and crosstalk just prior to impalements. At this time, the crack causes an extremely low resistance in one of the barrels, far less than the normal 20 MΩ.

Filling of the micropipette barrels with electrolyte is done as with a single barrel electrode. A small amount of electrolyte is injected into the blunt end of capillaries; 10 minutes later, the tip will have filled due to capillary action because of the internal filament. Even the glass twist will have filled. Backfilling of the bent barrel requires a fine gauge needle, so that it can be easily inserted past the bend right up to the twist.

3.1 Limitations

There are limitations to the use of double barrel micropipettes due to crosstalk and the localized nature of the current injection and voltage monitoring

3.1.1 Crosstalk between barrels

In a double barrel micropipette, the glass wall separating the two barrels is twice the thickness of the outer glass walls (Figure 5A). However, it is possibility that some current will 'leak' across the wall. The response of both barrels to a current injected through one barrel is shown in Figure 5B. There are voltage deflections in the second barrel. Initially, there is a capacitance spike due to capacitative coupling between the two barrels (Figure 5C), followed by a steady state deflection of very small magnitude. The deflection, expressed as a % coupling ($100 \bullet (\Delta E_2/\Delta E_1)$) is about 1–2% (Figure 5D).

3.1.2 Maximal current injection

As a consequence of the crosstalk between the two barrels, double barrel micropipettes are not suitable for measurements requiring large current injections. A 2 nA current causes a very small voltage deflection in the second barrel, but a µA current will cause a deflection large enough to affect measurements in walled cells, whose membrane potentials range from –50 to –200 mV. Thus, double barrel micropipettes are not suitable for measurements where µA currents are required, such as the large green algae *Chara* and *Nitella*, although larger micropipette apertures may be a solution.

3.1.3 Space clamping

Another problem associated with large cells is the incomplete 'spread' of voltage throughout the cell. When voltage clamping, the cell may not attain the specified voltage, this is incomplete space clamping. It is a problem for double barrel microelectrodes, because current injection and voltage monitoring occur in the same region within the cell. Incomplete space clamping should not be a problem for small, electrically isolated cells (such as guard cells). However, with large cells, or when there is electrical coupling between cells, the problem is pervasive. Under these conditions, quantitation requires multiple impalements, and correction depends upon assumptions about current spread and cell geometry. There is no simple authoritative solution. Examples of space clamping problems are shown for different cell types later in the chapter.

4 Use: Electronics and computer control

There are many resources describing electronics and computer control of experiments. Purves (1981) is a classic, still timely today. Ogden (1994) includes very useful contributions on microelectrodes, voltage clamping techniques and computer control. For versatility, we use digital oscilloscopes to monitor experiments and print a copy of recordings. For computer control: Analog/digital converters for measuring voltage and clamping currents, digital/analog converters for controlling the clamped voltage, digital input/output to switch voltage clamping on, and timers to control the duration of the voltage clamp are all supplied by a Labmaster board from Scientific Solutions (Solon, Ohio). The required software is written in C, compiled and run on a DOS computer. While this may seem anachronistic, the advantage for us is complete control of the experimental environment, including the CPU cycles of the computer. The technical specifications for hardware control have not changed, so newer systems offer little advantage. For new or experienced electrophysiologists, writing the software programs may be too daunting. If this is so, turnkey systems are available from many vendors at a significant cost. The latest development is the inclusion of a DSP (digital signal processor) chip in a stand alone system for performing measurements and voltage clamp.

4.1 Electrometers and voltage clamp circuit

Any electrometer with a sufficiently high input impedance ($>10^{11}$ Ω) will work. It is important to assure that the time responses of the voltage and current injecting headstages are the same, thus the input impedances should be matched. A voltage clamp circuit is connected to the electrometers. A schematic of the electronic circuit is shown in Figure 6.

5 Examples of measurements

Examples of measurements in walled cells can include any situation where current injection and voltage measurements must be kept separate. A variety of types of measurements in walled cells are described below. It is important to emphasize that, like any technique, double barrel micropipettes may not be sufficient to resolve the electrical properties of a cell. Some of these issues are outlined in the following examples.

5.1 Input resistance

By injecting a known current through one barrel, the magnitude of the voltage deflection in the other barrel can be used to calculate the resistance of the cell. If the geometry of the cell is known, than the specific resistance can be calculated. An example of such a measurement is shown in Figure 7, from a mesophyll cell of a *Ceratopteris richardii* gametophyte. In these cells, dye injected into the cell was distributed throughout the cytoplasm and did not migrate into adjacent cells, indicating that the impalement was cytoplasmic, and that cell-to-cell coupling was minimal. Having measured the mesophyll cell dimensions, the specific resistance could be calculated: about 1.5 $k\Omega \bullet cm^2$.

5.2 Current-voltage relations

An example of a current-voltage measurement using voltage clamping is shown in Figure 8, using trunk hyphae of the fungus *Neurospora crassa*. The measurement illustrates not only the voltage clamp technique, but also the issue of space clamping and time dependence. A hyphal compartment was impaled with a double barrel micropipette, and the same hypha impaled with a single barrel microelectrode at various distances from the first impalement. Although voltage fidelity was observed when the two micropipettes were within 10 microns of each other, current leakage through the plasma membrane causes an attenuated voltage clamp along the hypha. Cable theory can be used to correct for current attenuation in fungal hyphae (Gradmann et al. 1978; Lew, 2007).

5.3 Cell-to-cell coupling

An example of the use of double barrel micropipettes to measure electrical coupling through plasmodesmata is shown in Figure 9. The example is adjacent root hairs on an *Arabidopsis thaliana* root. Analogous to fungal hyphae, electrical connections between cells results in significant current passage into adjacent cells, resulting in an overestimate of the clamping current in voltage clamp measurements.

6. Summary

Electrophysiological analyses of ion transport in walled cells are essential to our understanding of the life of the cell. Ion transport plays crucial roles in regulating the intracellular milieu of the cell, in signal transduction, osmotic regulation and cellular growth. A detailed characterization of the electrical properties of the cells relies upon multiple techniques, among them, voltage clamping is very useful. Voltage clamping with double barrel micropipettes is especially important given the 'physiology problem' associated with patch clamp measurements on plasmolyzed protoplasts. Technical constraints and accessibility of the cell make voltage clamping a challenging endeavour, but double barrel micropipettes offer increased technical ease, simplifying the challenges faced by the researcher when working with intact cells. However, it should be clear from the examples presented in this chapter that double barrel micropipettes are not an absolute solution, but instead another step in our efforts to discover the roles of ion transport in cellular functions.

References

Ammann D (1986) Ion-selective microelectrodes. Principles, design and application. Springer-Verlag, Berlin, New York. pp 1–346

Blatt MR, Slayman CL (1983) KCl leakage from microelectrodes and its impact on the membrane parameters of a nonexcitable cell. J. Memb. Biol. 72:223–34

Blatt MR, Slayman CL (1987) Role of "active" potassium transport in the regulation of cytoplasmic pH by nonanimal cells. Proc. Natl. Acad. Sci. USA 84:2737–2741

Blatt MR (1987) Electrical characteristics of stomatal guard cells: the ionic basis of the membrane potential and the consequence of potassium chloride leakage from microelectrodes. Planta. 170:272–287

Blatt MR (1991). A primer in plant electrophysiological methods. In Methods in Plant Biochemistry. Volume 6. Assays for bioactivity. K. Hostettmann (ed.) Academic Press, London. (xi and 360 pages). pp. 281–321 (ISBN: 0124610161)

Bouteau F, Pennarun A-M, Kurkdjian A, Convert M, Cornel D, Monestiez M, Rona J-P, Bousquest U (1999) Ion channels of intact young root hairs from *Medicago sativa*. Plant Physiol. Biochem. 37:889–898

Etherton B, Higinbotham N (1960) Transmembrane potential measurements of cells of higher plants as related to salt uptake. Science 131:409–410

Etherton B, Keifer DW, Spanswick RM (1977) Comparison of three methods for measuring electrical resistances of plant cell membranes. Plant Physiol. 60:684–688

Finkel AS, Redman S (1984) Theory and operation of a single microelectrode voltage clamp. J. Neurosci. Meth. 11:101–127

Forestier C, Bouteau F, Leonhardt N, Vavasseur A (1998) Pharmacological properties of slow anion currents in intact guard cells of *Arabidopsis*. Application of the discontinuous single-electrode voltage-clamp to different species. Pflügers Arch. 436:920–927

Gradmann D, Hansen U-P, Long WS, Slayman CL, Warncke J (1978) Current-voltage relationships for the plasma membrane and its principal electrogenic pump in *Neurospora crassa*: Steady-state conditions. J. Memb. Biol. 39:333–367

Hamill OP, Marty A, Neher E, Sakmann B, Sigworth FJ (1981) Improved patch-clamp techniques for high-resolution current recording from cells and cell-free membrane patches. Pflügers Arch 391:85–100

Holdaway-Clarke TL, Walker NA, Overall RL (1996) Measurement of the electrical resistance of plasmodesmata and membranes of corn suspension-culture cells. Planta 199:537–544

Lew RR (1994) Regulation of electrical coupling between *Arabidopsis* root hairs. Planta. 193:67–73

Lew RR (2000) Electrobiology of root hairs. *In* Root Hairs. Cell and Molecular Biology. Ed. By Ridge RW, Emons AMC. Springer Verlag. Tokyo. pp. 115–139

Lew RR (2007) Ionic currents and ion fluxes in Neurospora crassa hyphae. J. Exp. Bot. 58:3475–3481.

Ogden D (ed.)(1994) Microelectrode Techniques. The Plymouth Workshop Handbook. The Company of Biologists, Cambridge. x + 448 pp

Purves RD (1981) Microelectrode Methods for Intracellular Recording and Ionophoresis. Academic Press, London. x + 146 pp

Raschke K, Shabahang M, Wolf R (2003) The slow and quick anion conductance in whole guard cells: their voltage-dependent alternation, and the modulation of their activities by abscisic acid and CO_2. Planta 217:639–650

Rall W (1977) Core conductor theory and cable properties of neurons. *In* Kandel, ER (ed.) Handbook of Physiology. Vol. 1 (Cellular Biology of Neurons, Part 1). American Physiological Society. Bethesda. pp 39–97

Roelfsema MRG, Steinmeyer R, Hedrich R (2001) Discontinuous single electrode voltage-clamp measurements: assessment of clamp accuracy in *Vicia faba* guard cells. J. Exp. Bot. 52:1933–1939

Slayman CL, Slayman CW (1962) Measurements of membrane potentials in Neurospora. Science 136:876–877

Thomas RC (1978) Ion-sensitive intracellular microelectrodes. How to make and use them. Academic Press, London, New York, San Francisco. xiii and 110 pp

Volkov AG (2006) Plant Electrophysiology. Theory and Methods. Springer-Verlag, Berlin Heidelberg. xxi and 508 pp.

Figure 1.
Construction of a single-barrel micropipette. A schematic of a typical set-up for pulling a micropipette is shown. The capillary glass is clamped in a stationary clamp above, and a moveable clamp below a heating element. As the glass melts, the lower clamp drops down; Initially by gravity alone, then with a strong pull (by activating a selenoid) to produce a sharp-pointed micropipette. The glass is borosilicate glass tubing with an internal filament; the internal filament assists filling with a conductive salt solution (usually 3 M KCl).

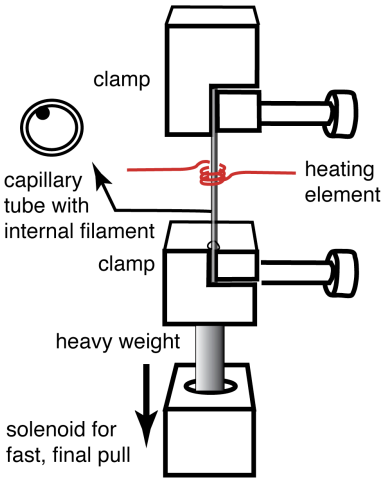

Figure 2.
Examples of intracellular impalements to measure the electrical properties of the cell. The three examples come from protists (**A**, the chlorophyte *Eremosphaera viridis*, bar=100 μm), fungi (**B**, the ascomycete *Neurospora crassa*, bar=20 μm) and a higher plant (**C**, *Arabidopsis thaliana*, bar = 20 μm). Examples of the electrical responses to impalement are also shown. In the impalement of *E. viridis* (**A′),** the voltage rapidly becomes negative, and then slowly becomes even more hyperpolarized, probably due to slow sealing at the impalement site. The examples for *N. crassa* (**B′**) and *A. thaliana* (**C′**) are both dual impalements. The second impalements (starred arrows) have no effect on the measured voltage. This indicates the high resistance at the impalement site; so high that shunt leakage does not cause a depolarized potential. Additional evidence for the electrical integrity of the seal at the impalement site is demonstrated in the micropipette removal from the *N. crassa* hypha. The high turgor causes blowout of cytoplasm from the hypha, but only after removal. Thus the seal at the impalement site resists pressures as high as about 600 kiloPascal.

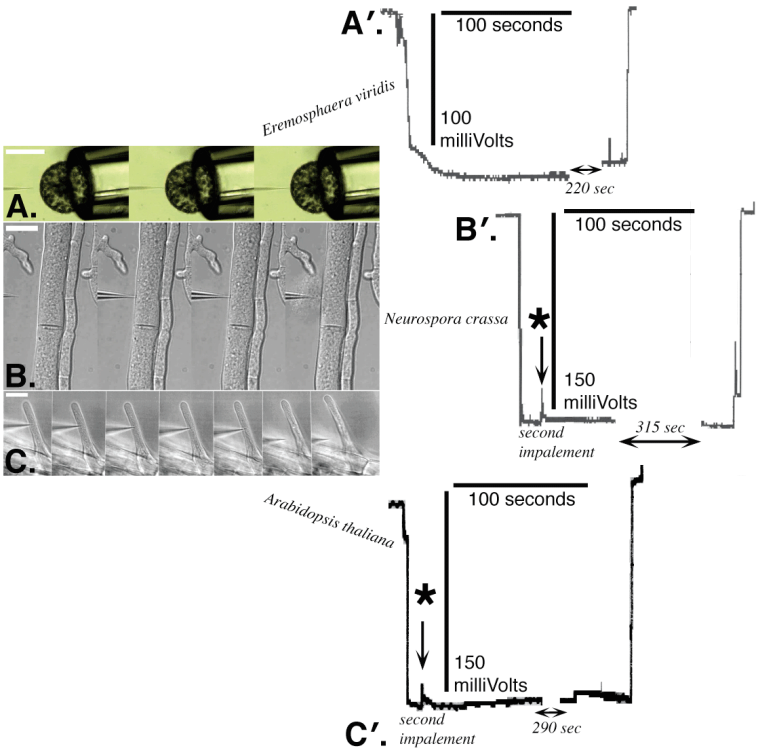

Figure 3.
Idealized electrical network of a walled cell. Resistances and capacitance and the potential are shown for both the plasma membrane and vacuole. The potential of the plasma membrane is usually in the range of 100-200 mV, negative-inside. The vacuole is about 20 mV, positive-inside. Capacitance of either membrane depends on the area, specific capacitance is about 10^{-2} Farads m^{-2} for biological membranes.

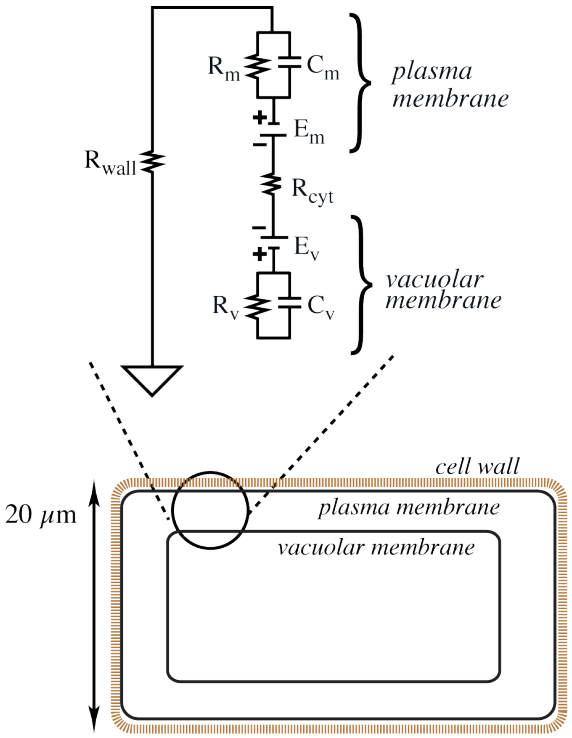

Figure 4.
Construction of a double barrel micropipette. **A**. First, the two capillaries —held together by clamps above and below a heating element (1)— are heated in a localized region. When the glass has softened, the two capillaries are twisted by rotating one of the clamps 360º (2). The two capillaries are then pulled to form the sharp tip (3), and removed from the pipette puller. **B**. A drop of fast-setting epoxy is applied to the joint between the two barrels at the fused twist to strengthen the joint (4). Finally, one of the capillaries is softened by localized heating and pulled away to produce a Y-shape (5). The photo inset (**C**) shows the two capillaries, twisted together in the second panel, pulled in the third panel, and after final fabrication in the fourth panel. Bar=2 cm.

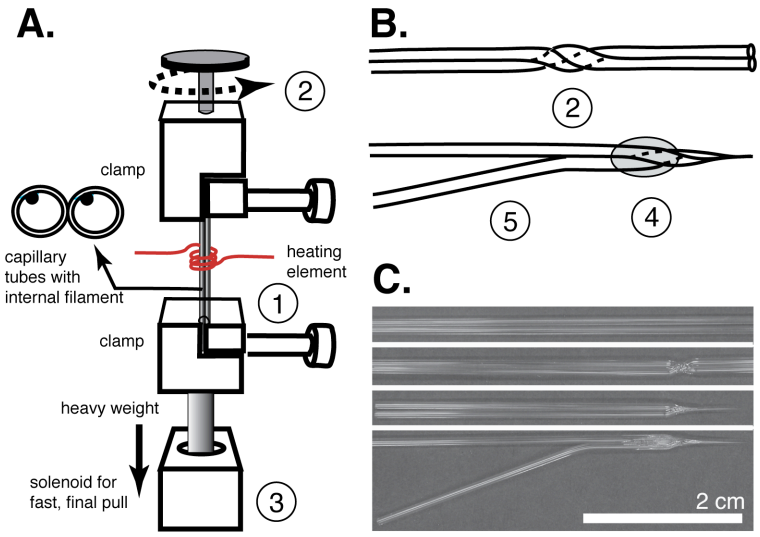

Figure 5.
Electrical properties of the double barrel micropipette. **A**. Scanning electron microscopy of double barrel micropipette tip (*left*. tip shape; *right*. tip apertures). Note the double thickness of glass between the two apertures. Bars 4.3 and 0.5 µm, as shown. **B**. Voltage response of the two barrels (E_1 and E_2) to a 2 nA peak to peak current injected into the first barrel (E_1). The large voltage deflection in the first barrel is due to the resistance of the micropipette tip, 25 MΩ in this example. Some of the current 'leaks' across the glass barrier between the two barrels, causing a much smaller voltage deflection in the second barrel (E_2, about 1 mV). Spikes at each step transition in the current injection are caused by the capacitance of the glass barrier between the two barrels. The measurements were performed with 3 M KCl filling the barrels, and 150 mM KCl in the external solution to mimic the ionic conductivity of the cytoplasm. Grounding was with a chlorided silver wire. The resistive network is shown in **C**. By measuring the resistance of each barrel, and the amount of 'coupling' between the barrels ($100 \bullet (\Delta E_2/\Delta E_1)$)(**D**), it was possible to estimate the value of the resistance of the glass barrier between the two barrels. The value ranged from 500 MΩ to 100 GΩ, the median value was 3 GΩ. This is consistent with the known resistivity of borosilicate glass, about 10^{15} Ω•cm. With an estimated barrier thickness of 100 nm, the calculated resistance would be 10 GΩ.

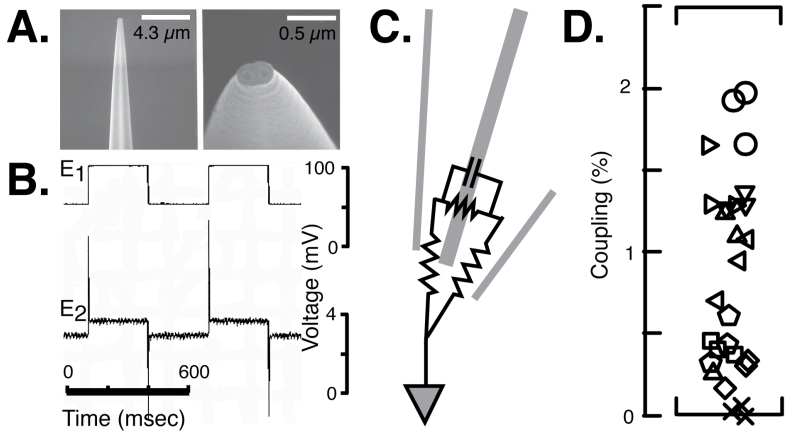

Figure 6.
Voltage clamping schematic. **A**. If we specify $V_{Command}$, the operational amplifier will drive whatever current is necessary into the feedback system (the cell and feedback resistor $R_{Feedback}$) to maintain V_{Cell} at $V_{Command}$. **B**. A more detailed equivalent circuit. The $TTL_{I/O}$ is a switch relay controlled by the computer to turn on the voltage clamping circuit. The V_{Cell} is measured at the electrometer ($V_{Monitor}$). The current is injected via the $I_{Stimulus}$ input of another electrometer. The feedback resistor in this example is very high (125 MΩ) and assures a fast response by the operational amplifier so that V_{Cell} is rapidly clamped with high fidelity.

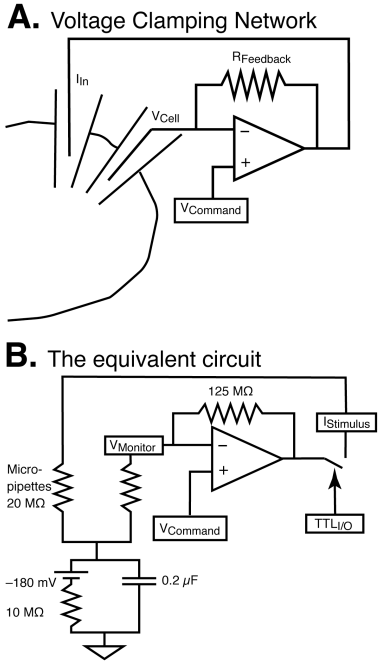

Figure 7.
Input resistance measurements from a mesophyll cell of *Ceratopteris richardii*. Both voltage (top trace) monitored with one barrel of the double barrel micropipette and current (lower trace) injected through the other barrel are shown. Prior to and after the experiment, electrode tests were conducted to assure there was no electrical crosstalk between the voltage monitoring and current injecting electrodes. Current injection through the voltage-monitoring electrode causes a voltage deflection as expected, but current injection through the current-injecting electrode caused no visible deflection in the voltage-monitoring electrode. Immediately following impalement, confirmed visually, a transient negative spike is followed by a slow sealing event that is characterized by a gradual hyperpolarization to a stable potential. After impalement, current injection through one barrel of the double barrel micropipette causes a voltage deflection in the other barrel due to the resistance of the plasma membrane. This confirmed that the impalement was successful. The response of the cell to changes in photosynthesis are documented in this experiment. Removal of the pipette from the cell results in a rapid depolarization to a value similar to what was observed before the cell was impaled.

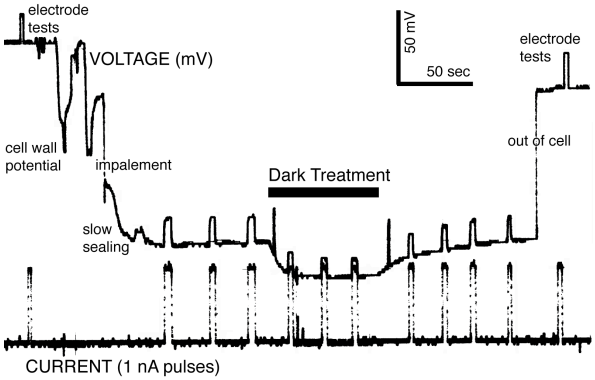

Figure 8
Current-Voltage measurements: The effect of cable properties. The example is for hyphal trunks of the fungus *Neurospora crassa*. **A**. examples of impalements with varying distances between impalement sites. One of the micropipettes was double-barreled, the other single barrel. Voltage clamping was performed with the double barrel microelectrode, and voltage deflections in the single barrel microelectrode used to determine the magnitude of voltage attenuation (V_d/V_0 where V_d is the voltage measured with the single barrel microelectrode and V_0 the voltage measured with the double barrel microelectrode). **B**. Time dependent changes in clamping current were complete within 100 msec. **C**. The voltage attenuation can be fit to an exponential function to determine the length constant for the hypha —the degree of voltage attenuation, which will depend upon the extent of current leakage out of the hypha as distance increases: $V_d/V_0 = e^{(x/-\lambda)}$, where x is the separation distance and λ is the length constant. To correct for current attenuation and obtain current density (I_m in units of A m^{-2}), the cable current (i_m in units of A m^{-1}) is calculated ($i_m = I/2\lambda$, where I is the current, and the term 2λ accounts for the current attenuation in both directions), then the current density ($I_m = i_m/(\pi d)$, where (πd accounts for the effect of hyphal diameter) (Rall, 1977; Lew, 2007).

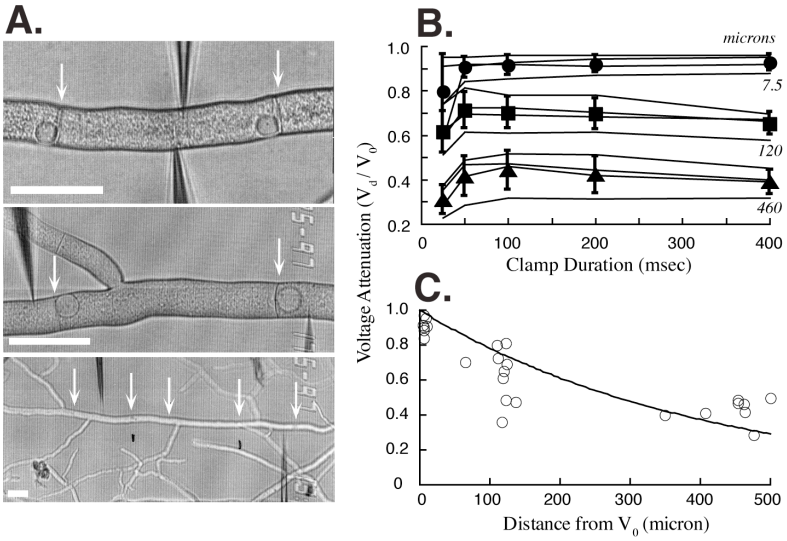

Figure 9.
Example of cell-to-cell coupling measurement. This example is for two root hairs adjacent to each other on a longitudinal file of an *Arabidopsis thaliana* root. **A**. diagrammatic representation of cell-to-cell coupling through plasmodesmata. **B**. As marked, $Cell_1$ is impaled with a double-barrel electrode, followed by a separate impalement into $Cell_2$. A 5 nA pulse through the current-injecting electrode in $Cell_1$ results in a voltage deflection in both $Cell_1$ and in $Cell_2$, due to coupling through plasmodesmata. **C**. A higher magnification segment of the traces shown in A. C. Regulation of cell-to-cell coupling between root hairs was described by Lew (1994).